Chapter 6

Modeling Biomass Substrates for Syngas Generation by Using CFD Approaches

Nuno Couto and Valter Silva

Additional information is available at the end of the chapter

http://dx.doi.org/10.5772/65857

Abstract

Recent reports from top universities state that in spite of having great national importance, there are dozens of fields of study that are suffering due to a lack of funding. Perhaps the greatest tool available to assist researchers with this regard is numerical simulation. This tool allows cutting costs, decreasing the necessary design cycle and allows an enormous amount of physical insight on the process itself). Numerical model's ability to correctly predict a complex system was tested in this chapter by drawing from a previously developed computational fluid dynamics model for biomass gasification. Numerical results were compared with both experimental results (pilot scale plant) and available literature. Results from common Portuguese biomass substrates were found to be within a satisfactory margin of error of 20%. Influence of all major operational conditions was then investigated and the model was once again able to predict all the expected trends. All the relevant process products were also analyzed. Finally, the numerical model was coupled with an optimization model. Maximum efficiency value was found at 900°C with a SBR of 1.5 for MSW and 1 for forest residues. Results showed that numerical models could have a preponderant impact on biomass gasification field.

Keywords: numerical simulation, biomass, municipal solid wastes, gasification, optimization

1. Introduction

In the last few years, biomass has become an important source of energy and it most often refers to any organic matter derived from plant-based materials. Biomass includes, among others, forestry and agricultural residues, organic waste, energy crops, sewage sludge, and woody plants [1, 2].

Among all the thermochemical conversion processes, gasification has been emerging as a very promising technology due to being environmental friendly, having high efficiency and flexible

enough to use different substrates with a wide range of applications for heat, electricity, chemicals, and transportation purposes [3]. Gasification can be defined as the conversion of a solid waste to synthetic gas or fuel by the partial oxidation of the feedstock under stoichiometric combustion conditions. The synthetic gas is generally called "producer gas" or syngas and contains mainly carbon monoxide and hydrogen. However, some undesired products can be also found such as tar, alkali metals, chloride and sulfide, among others [3]. Gasification presents several advantages over waste combustion, namely and among others [3]: (a) effective response to increasingly environmental restrictive regulations; (b) syngas can be used not only in highly efficient internally fired cycles but also in producing valuable products as chemicals and fuels; and (c) flexible use under different operating conditions and reactors.

However, some drawbacks need further investigation. Besides high ranges of operating and capital costs than those of conventional combustion-based plants, the syngas generated from biomass and especially from municipal solid wastes (MSWs) gasification is unstable due to changes in the feedstock properties. Indeed, the high heterogeneous nature of MSW implies significant variations in syngas yield and quality [4]. The negative impact from the heterogeneous nature of MSW can be reduced by implementing strategies as MSW preprocessing, where undesired MSW components are removed before sending them to the gasifier. Further improvements can also be found by blending MSW with other feedstock with more favorable characteristics [5]. Portugal has a major potential considering biomass resources, only forestry and pruning residues have potential to produce 13,800 GWh, about 13% of the total primary energy demand in Portugal [6]. Also, operating the MSW gasifier under certain operating conditions will allow reliable operation with stable and improved syngas generation.

Because experimental runs conducted on industrial gasification plants or even on pilot scale gasification plants are very expensive, predictable models able to simulate the syngas composition and other responses of interest are required. Accurate predictions by gasification models require the simulation of different kinetic and hydrodynamic phenomena and we should not forget that gasification always involves complex chemistry. Concerning this degree of complexity, and also, the high investment costs involved to perform the experimental studies, the use of tools involving numerical simulation, such as computer fluid dynamics (CFD), exhibit utmost importance [7–9].

There are different designs to build a gasifier but one with special relevance is the fluidized bed configuration [10]. Basically, in this kind of reactor, both fuel and inert bed material act as a fluid. To obtain this behavior a gas is forced to pass through the solid particles of the reactor. The great advantages of operating such a system are its ability to handle with different feedstock due to the easy control of temperature, to deal with fine grained materials and the fact that generates an intense mixing enhancing the transference of mass and heat. Finally, the fluidized bed gasifiers are flexible enough to use additives with the goal to remove pollutants and increase tar conversion [11].

The fluidized bed gasification is essentially a multiphase problem. There are two main strategies that are commonly implemented to handle this kind of gasification: Euler-Lagrange and Euler-Euler approaches [12]. In the Euler-Lagrange strategy, the dispersed phase is characterized by following a wide number of particles through information given from the continuum

http://dx.doi.org/10.5772/65857

phase. Both phases exchange mass, momentum, and energy. One major assumption relies on the fact that volume fraction of the dispersed phase is lower than about 10%, even the mass fraction could be higher.

Snider et al. [13] implemented a 3-D model based on the previous approach to simulate the behavior of a coal gasifier. The model also included energy transport equations and homogeneous and heterogeneous chemistry described by reduced chemistry. The model was able to identify zones with stagnant particles and then provide important data for reactor design purposes.

The Euler-Euler approach considers the different phases as interpenetrating continua, meaning that both volume phases depend on each other regarding time and space. Each phase obeys the conservation laws and constitutive relations from empirical data are required to close the equations system. Regarding the Euler-Euler approach, there are three multiphase models: (a) the volume of fluid; (b) the mixture model and; (c) the Eulerian model, which is indicated to model the discussed gasification system in this chapter.

Xue et al. [14] followed the Eulerian-Eulerian approach to predict the syngas generation from wood gasification using air as a fluidization agent. The developed model was able to provide detailed information on several processes, such as char elutriation, species profiles along the reactor and gas composition at reactor outlet.

This work aims at presenting an advanced modeling strategy within the framework of the CFD ANSYS Fluent program combined with suitable experimental data input and user defined the code to predict a gasification process under several operating conditions and robust enough to be applied both to biomass and MSW. Model development is detailed highlighting the set of complex choices that have to be taken and corresponding implications and consequences. Numerical results for both biomass and MSW were validated against experimental results, and then, the effect of using different operating conditions is deeply discussed as well as the main syngas quality indices. The combined use of the developed numerical model and the design of experiments (DoE) procedure is also discussed for optimization purposes. Finally, a reflection section is included to highlight the efficiency and effectiveness of using numerical methods to describe physical problems.

2. Experimental setup

The numerical model (presented in Section 3) was developed using experimental data collected in the gasification plant from the School of Technology and Management (ESTG) of the Polytechnic Institute of Portalegre (IPP). The plant is based on fluidized bed technology, with a 200 kW reactor that produces an average syngas flow rate close to 100 Nm^3/h. **Figure 1** depicts a diagram of the biomass gasification unit used in the experiments.

The system comprises two biomass silos connected to a worm screw, which forms the feeding system. The gasifier itself is just slightly above 4 m high and half a meter wide with a biomass intake capacity of 100 kg/h. The synthetic gas is cooled by two heat exchangers, with the first

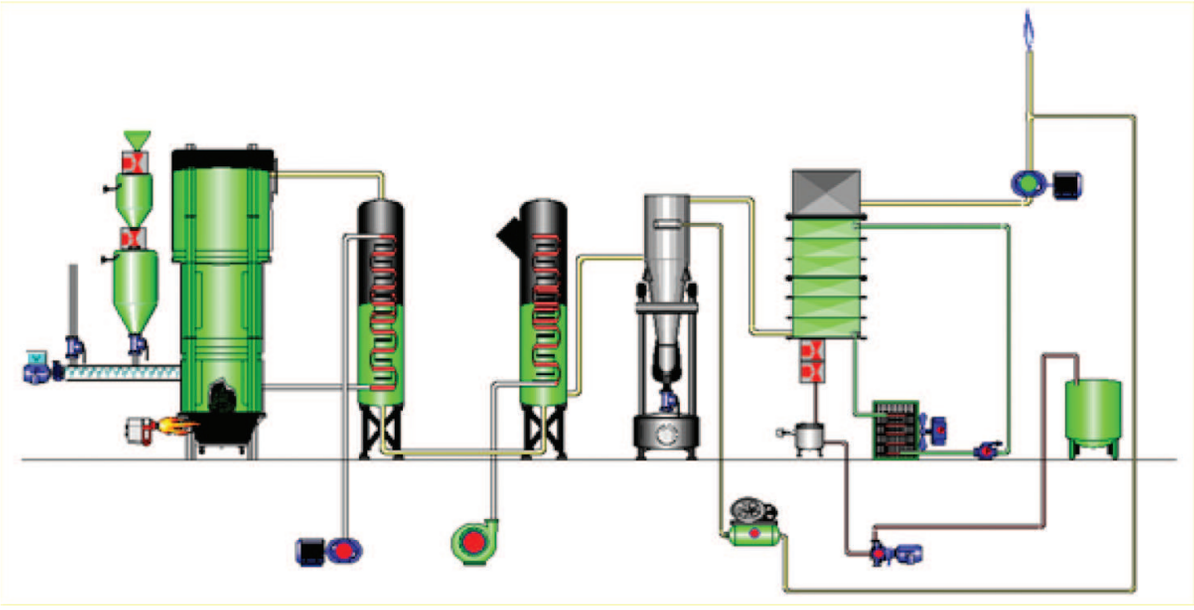

Figure 1. Schematics of the gasification plant.

one being also responsible for preheating the gas. The ash and char are removed to the bag filter, a system with seven filters cleaned with shots taken from synthetic gas through a compressor downstream of the vacuum pump. The purpose of the third heat exchanger is to remove tars from the system by condensation, which are then forwarded to a deposit. The last component of the system is a vacuum pump, which guarantees that the entire system control.

Once the predetermined temperature and biomass input flow are secured, the system stabilizes for about 2 h and then the test starts. The test lasts 2 h each, including syngas collections (usually taking two different samples) and recording temperatures, flows, ash, and tars. The schematics as well as an extensive description of the gasification plant can be found elsewhere [15, 16].

The described system was first used to analyze the gasification process of Portuguese biomass substrates and their potential for fossil fuel replacement [15, 17]. Recently, to counter the improper disposal of municipal waste in landfills, the focus shifted from Portuguese biomass gasification to Portuguese municipal solid waste (referred from now on as PMSW for simplicity) gasification.

The characterization and analysis of Portuguese MSW were carried out using data from the Oporto metropolitan area obtained from LIPOR, entity responsible for the management, treatment, and recovery of solid waste municipal produced in the city. From the pretreatment of MSW conducted by LIPOR, usually via shredding and dehydration, a refuse-derived fuel (RDF) containing only cellulosic and plastics is obtained [18] (chemical composition of the MSW is presented in **Table 1**).

However, since at that moment, the reactor could not handle LIPOR's wastes, the model had to be validated using data collected from the literature. To properly assess the potential of PMSW,

http://dx.doi.org/10.5772/65857

Category	% Weight	Chemical formula
Cellulosic material	85.42	*
Polyethylene	10.99	$(C_2H_4)_n$
Polyethylene terephthalate	2.02	$(C_{10}H_8O)_n$
Polypropylene	0.81	$(C_3H_6)_n$
Polystyrene	0.76	$(C_8H_8)_n$

Table 1. Chemical composition of the MSW in Oporto in 2014.

Substrate properties	Forest residues	PMSW
Elementary analysis (dry ash free)		
N (%)	2.4 ± 0.3	1.4 ± 0.2
C (%)	43 ± 4.1	48 ± 4.4
H (%)	5 ± 0.6	6.3 ± 1.4
O (%)	49.6 ± 5.2	43.6 ± 3.6
Humidity (%)	11.3 ± 1.7	17.6 ± 2.3
Density (Kg/m^3)	650 ± 70	247 ± 23
Lower heating value (MJ/Kg biomass)	21.2 ± 1.8	14.4 ± 1.1
Mean particle size (mm)	5 ± 2	20 ± 10
Proximal analysis (%)		
Ash	0.2 ± 0.1	14.9 ± 1.2
Volatile matter	79.8 ± 3.1	76.62 ± 2.9
Fixed carbon	20 ± 2.5	8.46 ± 1.5

Table 2. Ultimate and proximate analyses of forest residues and PMSW.

a previously studied Portuguese biomass substrate will be used as benchmark. Forest residues [17] (in pellet form) were selected for this purpose, since it revealed relevant energetic as well as economic benefits.

Prior to the actual gasification process, biomass analysis was carried out in the Laboratory of Chemistry of the High School of Technology and Management located in Portalegre, Portugal, since biomass characteristics can provide valuable information on how the gasification process will occur. This kind of analysis also provides crucial data to treat the implemented numerical model. The instruments used in the performed analysis are: thermal gravimetric analysis—data for proximal analysis; elemental analysis—determination of biomass composition with respect to the percentage of C, H, N, and O; humidity—sample moisture content assessment; calorific value—appraisal of energy contained in biomass. Data regarding proximate and ultimate analysis for the referred substrates are presented in **Table 2**.

It should be noted that regarding the experimental gasification runs, as well as the analyses for the studied substrates, every run was performed twice in order to avoid measurements. When

deviation was higher than 5%, extra runs were performed to ensure reproducibility below 5%, which is typical for this kind of system.

3. Mathematical model

Experimental studies conducted in pilot scale or industrial reactors like the one presented in the previous section are fairly absent from the available literature. The reason is due to the difficulty in regulating operating parameters but primarily due to the high cost of a gasification plant, which can reach tens of millions of Euros depending on the generated power [19].

Mathematical models, with the ability to theoretically simulate any physical condition, allow studying the gasification process without resorting to major investments and/or the need for long-waiting periods (with all the bureaucratic and logistical problems associated). However, due to the extreme complexity of the gasification process, largely due to the chemical and physical interactions that occur throughout, the ability of numerical models to correctly predict experimental data collected from pilot scale or industrial reactors is usually very limited. In fact, the lack of reliable models to describe the gasification process in the open literature was the main motivation for our team to develop a new CFD model able to predict the syngas generation from biomass gasification in a pilot scale gasifier [20].

3.1. Gas-solid interaction

When modeling bubbling fluidized-bed reactors, like the one described, the two-phase flow theory of fluidization is usually applied for the description of the process hydrodynamics. Because of this, correctly modeling the interaction between gas and solid phases is crucial since they exchange heat by convection, mass over the heterogeneous chemical reactions, and momentum due to the drag between gas and solid phase. The main equations governing both phases are depicted in **Table 3**.

3.1.1. Granular Eulerian model

According to Goldschmidt et al. [21], two-phase flows can be modeled using two different approaches: the Lagrangian-Eulerian and the Eulerian-Eulerian models. With considerable similarities, the fundamental difference between them lies in the way the particles are treated. The former describes the solid phase at the particle level while the latter treats the particles as a continuum. In industrial applications, typically composed of millions of particles, following individual particles become excessively time consuming and for this reason the Lagrangian approach tends to be less used [22].

The Eulerian approach not only requires lower computational resources and calculation times, but also allows a detailed analysis of the disperse phase flow field, which is convenient for engineering design applications. For this reason, the granular Eulerian model was applied to our model.

Gas phase	Solid phase
Energy:	
$\frac{\partial(\alpha_g \rho_g h_g)}{\partial t} + \nabla \cdot (\alpha_g \rho_g \vec{u}_g h_g) = -\alpha_g \frac{\partial(p_g)}{\partial t}$ $+\overline{\overline{\tau}}_g : \nabla(\vec{u}_g) - \nabla \vec{q}_g + S_g + \sum_{g=1}^{n} (\vec{Q}_{sg} + \dot{m}_{sg} h_{sg})$	$\frac{\partial(\alpha_s \rho_s h_s)}{\partial t} + \nabla \cdot (\alpha_s \rho_s \vec{u}_s h_s) = -\alpha_s \frac{\partial(p_s)}{\partial t}$ $+\overline{\overline{\tau}}_s : \nabla(\vec{u}_s) - \nabla \vec{q}_s + S_{ps} + \sum_{s=1}^{n} (\vec{Q}_{sg} + \dot{m}_{sg} h_{sg})$
Mass:	
$\frac{\partial(\alpha_g \rho_g)}{\partial t} + \nabla \cdot (\alpha_g \rho_g \vec{u}_g) = -M_C \sum \gamma_C R_C$	$\frac{\partial(\alpha_s \rho_s)}{\partial t} + \nabla \cdot (\alpha_s \rho_s \vec{u}_s) = M_C \sum \gamma_C R_C$
Momentum:	
$\frac{\partial(\alpha_g \rho_g \vec{u}_g)}{\partial t} + \nabla \cdot (\alpha_g \rho_g \vec{u}_g \vec{u}_g) = -\alpha_g \nabla p_g + \alpha \rho_g g$ $+\beta(u_g - u_g) + \nabla \cdot \alpha_g \overline{\overline{\tau}}_g + S_{sg} U_S$	$\frac{\partial(\alpha_s \rho_s \vec{u}_s)}{\partial t} + \nabla \cdot (\alpha_s \rho_s \vec{u}_s \vec{u}_s) = -\alpha_s \nabla p_s + \alpha \rho_s g$ $+\beta(u_s - u_s) + \nabla \cdot \alpha_s \overline{\overline{\tau}}_s + S_{sg} U_S$

Table 3. Governing equations for gas and solid phases.

The granular Eulerian model is described by the following conservation equation for granular temperature:

$$\frac{3}{2}\left[\left(\frac{\partial(\rho_s \alpha_s \Theta_s)}{\partial t}\right) + \nabla \cdot (\rho_s \alpha_s \vec{v}_s \Theta_s)\right] = (-p_s \bar{I} + \overline{\tau}_s) : \nabla(\vec{v}_s) + \nabla \cdot \left(k_{\Theta_a} \nabla(\Theta_s)\right) - \gamma_{\Theta a} + \phi_{ls} \qquad (1)$$

This expression is obtained from the kinetic theory of gases. The term $(-p_s \bar{I} + \overline{\tau}_s) : \nabla(\vec{v}_s)$ describes the generation of energy by the solid stress tensor, ϕ_{ls} stands for the energy exchange between the fluid and solid phase, γ_{Θ_a} stands for the collisional dissipation of energy and $k_{\Theta_a} \nabla(\Theta_s)$ stands for the diffusion energy, in which k_{Θ_a} is the diffusion coefficient.

3.2. Turbulent model

In turbulent flows, like the one being studied, transported quantities like momentum, energy, and species concentration tend to fluctuate. Modeling fluctuations can be to computationally expensive, which is why instantaneous governing equations are usually replaced with their time-averaged, ensemble-averaged, or otherwise manipulated to remove the small time scales.

The standard k-ε model was used to simulate the turbulent flow due to its suitability for a wide range of wall-bounded and free-shear flows. The model is the simplest turbulence two-equation model in which the solution of two separate transport equation allows the turbulent velocity and length scales, which are to be independently determined. Turbulence kinetic energy (k) and dissipation rate (ε) are, respectively, given by:

$$\frac{\partial}{\partial t}(\rho k) + \frac{\partial}{\partial x_i}(\rho k u_i) = \frac{\partial}{\partial x_j}\left[\left(\mu + \frac{\mu_t}{\sigma_k}\right)\right] G_k + G_b - \rho\varepsilon - Y_M + S_k \quad (2)$$

$$\frac{\partial}{\partial t}(\rho \varepsilon) + \frac{\partial}{\partial x_i}(\rho \varepsilon u_i) = \frac{\partial}{\partial x_j}\left[\left(\mu + \frac{\mu_t}{\sigma_\varepsilon}\right)\right] + C_{1\varepsilon}\frac{\varepsilon}{k}(G_\varepsilon + C_{3\varepsilon}G_b) - C_{2\varepsilon}\rho\frac{\varepsilon^2}{k} + S_\varepsilon \quad (3)$$

To determine the turbulence kinetic energy as well as the dissipation rate, the following constants were assumed: G_k = 1.0 and G_ε = 1.3 stand for the turbulent Prandtl numbers for k and ε, respectively, $C_{1\varepsilon} = 1.44$, $C_{2\varepsilon} = 1.92$, and $C_{3\varepsilon} = 0$ are default constants commonly used in fluent and S_k and S_ε are user-defined source terms.

3.3. Chemical reaction model

In this study, two different chemical reaction models were used in the simulation: the finite-rate/Eddy-dissipation model was used to describe homogeneous reactions while the kinetic/diffusion surface reaction model was employed for heterogeneous ones. The main distinction between these two models is associated with how the carbon species are treated. The homogeneous gas reaction assumes the carbon species gasified straightaway, and that the carbon is treated as a gas, while heterogeneous particle-gas reaction treats carbon as solid particles and they go through finite-rate reaction via a typical reaction at particle surface. **Table 4** presents the main reactions as well as the corresponding reaction rates for these two models.

Above reactions can slightly change if different gasifying agents other than air are considered. Previously published models using steam [23] and carbon dioxide [24] address those exact changes.

Reactions	Reaction rate
Homogeneous reactions:	
$CO + 0.5O_2 \rightarrow CO_2$	$r_1 = 1.0\times10^{15}\exp\left(\frac{-16,000}{T}\right)C_{CO}C_{O_2}^{0.5}$
$CO + H_2O \rightarrow CO_2 + H_2$	$r_2 = 5.159\times10^{15}\exp\left(\frac{-3430}{T}\right)T^{-1.5}C_{O_2}C_{H_2}^{1.5}$
$CO + 3H_2 \leftrightarrow CH_4 + H_2O$	$r_3 = 3.552\times10^{14}\exp\left(\frac{-15,700}{T}\right)T^{-1}C_{O_2}C_{CH_4}$
$H_2 + 0.5O_2 \rightarrow H_2O$	$r_4 = 2780\exp\left(\frac{-1510}{T}\right)\left[C_{CO}C_{H_2O} - \frac{C_{CO_2}C_{H_2}}{0.0265\exp\left(\frac{3968}{T}\right)}\right]$
$CH_4 + 2O_2 \rightarrow CO_2 + 2H_2O$	$r_5 = 3.0\times10^{5}\exp\left(\frac{-15,042}{T}\right)C_{H_2O}C_{CH_4}$
Heterogeneous reactions:	
$C + 0.5O_2 \rightarrow CO$	$r_6 = 596T_P\exp\left(\frac{-1800}{T}\right)$
$C + CO_2 \rightarrow 2CO$	$r_7 = 2082.7\exp\left(\frac{-18,036}{T}\right)$
$C + H_2O \rightarrow CO + H_2$	$r_8 = 63.3\exp\left(\frac{-14,051}{T}\right)$

Table 4. Chemical reaction model.

http://dx.doi.org/10.5772/65857

3.4. Model expansion for MSW

In the above subsection, we purposely did not address the mathematical treatment for the devolatilization phenomenon. The reason why being that the devolatilization section was only properly included when the model was expanded to handle the heterogeneity of MSW. Until that point, a single rate model, developed by Badzioch and Hawksley [25], was assumed which computed reliable devolatilization rates in a simple way.

To cope with the heterogeneity of said substrate a pyrolysis model with secondary tar generation was implemented. MSW is mainly composed of cellulosic and plastic components, and while cellulosic material can be divided in cellulose, hemicellulose, and lignin [26], plastics comprise polyethylene, polystyrene, and polypropylene, among others. To distinguish the several components that comprise the MSW, the pyrolysis reactions of cellulosic and plastic groups are considered individually and following an Arrhenius kinetic expression, as shown in **Table 5**.

3.5. Numerical procedure

Fluent, a finite volume method-based CFD solver, was employed in this work to solve the stated problem. Regarding the geometry modeling there are some simplifications that one can make in order to make the computation less expensive. Since the described reactor type is cylindrical, one can use a 2D axisymmetric problem setup.

Mesh was built using GAMBIT software and a total number of 83,000 quadrilateral cells of uniform grid spacing were generated. The mesh density in a finite element model is an important topic because of its relationship to accuracy and cost. In this particular case, the chosen cell size was about 12 times larger than the average particle size which was shown to be able to effectively capture the hydrodynamics in fluidized bed gasifier [27].

In such a complex model, it is sometimes difficult to define a good initial condition. For this reason, the process was first simulated considering only flow and nonreacting heat transfer (also known as "cold flow") and after reaching conversion reactive multiphase flow was added.

Substrate and air inlet were defined as "velocity inlets". Each velocity-inlet surface was identified by mass fractions, temperature, and a velocity magnitude. The flow direction was kept normal to

Reactions	Reaction rate
Cellulose $\rightarrow \alpha_1$volatiles $+ \alpha_2 TAR + \alpha_3$char	$r_9 = A_i \exp\left(\frac{-E_i}{T_s}\right)(1-a_i)^n$
Hemicellulose $\rightarrow \alpha_4$volatiles $+ \alpha_5 TAR + \alpha_6$char	$r_{10} = A_i \exp\left(\frac{-E_i}{T_s}\right)(1-a_i)^n$
Lignin $\rightarrow \alpha_7$volatiles $+ \alpha_8 TAR + \alpha_9$char	$r_{11} = A_i \exp\left(\frac{-E_i}{T_s}\right)(1-a_i)^n$
Plastics $\rightarrow \alpha_{10}$volatiles $+ \alpha_{11} TAR + \alpha_{12}$char	$r_{12} = \left[\sum_{i=1}^{n} A_i \exp\left(\frac{-E_i}{RT}\right)\right]\rho_v$
Primary$TAR \rightarrow$ volatiles $+$ *S*econdaryTAR	$r_{13} = 9.55\times10^4 \exp\left(\frac{-1.12\times10^4}{T_g}\right)\rho_{\mathrm{TAR1}}$

Table 5. Devolatilization model.

the surface. Turbulence of the inlet surfaces was detailed by turbulence intensity and hydraulic diameter. Outlet was set as the pressure outlet, specified by a gauge pressure value of zero.

For the pressure-velocity coupling, the widely used SIMPLE algorithm was enabled. For all simulations presented in this paper, a first-order upwind scheme was used for all equations. The standard scheme was used for interpolation methods of pressure. This means that the solution approximation in each finite volume was presumed to be linear, leading to less computational expenses. In order to properly justify using a first-order scheme, it was necessary to make sure that the grid used in this work had adequate resolution to accurately capture the physics occurring within the domain. In other words, the results needed to be independent of the grid resolution. Nonetheless, for better accuracy, this was later changed to the second-order upwind scheme.

Similarly, the underrelaxation factors were initially set at 0.5 (except for turbulent viscosity, pressure, and body forces, which were kept the same as default), and were then gradually conveyed to their default values with convergence. Convergence criteria were set that normalized residuals for all equations must fall under 10^{-6}.

4. Results and discussion

4.1. Model validation for forest residues

The main goal of researchers when it comes to numerical simulation is to increase the system complexity and accuracy while minimizing, if not complete eliminating, physical testing. There are two key systematic processes for confirming numerical results: the verification and the validation processes. The former tries to answer "did I solve the model right?" while the latter asks "did I solve the right model?" and this is where one checks against experimental data.

In the gasification process, this step becomes crucial since one is dealing with an extremely complex multiphase model where gas and solid phases exchange heat, momentum, and mass. To make matters worse, the hydrodynamic phenomena on a laboratory scale fluidized bed are not the same as on large scales [28]. To overcome this problem, the numerical results were compared with gasification tests performed in a pilot scale gasification plant, installed in the Industrial Park of Portalegre, Portugal. A wide range of operational conditions were tested for several Portuguese biomass substrates. **Table 6** shows three of these tested operating conditions for one particular substrate used to validate the numerical model and respective results.

The presented results show that the developed numerical model has the ability to predict the obtained synthetic gas composition within a satisfactory margin of error of 20%, commonly found in similar studies [29]. The highest deviation was observed for CH_4, which was expected since smaller fractions tend to produce higher relative errors. Furthermore, all light hydrocarbons and tar can lump into CH_4, which can explain the disagreement sometimes found in Ref. [15]. Very similar margins of error were found for different biomass substrates analyzed in the same pilot scale.

Nevertheless, some differences can be observed due to some simplifying assumptions followed by our model:

http://dx.doi.org/10.5772/65857

Experimental conditions		Forest residues		
Run		1	2	3
Temperature (°C)		815	815	790
Admission biomass (Kg/h)		63	74	63
Air flow rate (Nm^3/h)		94	98	98
Syngas fraction (dry and inert basis)				
H_2	Experimental	8.2	8.4	7.6
	Numerical	7.5	7.7	6.8
CO	Experimental	18.6	18	17.9
	Numerical	20.9	20.6	20.1
CH_4	Experimental	4.6	4.4	4.4
	Numerical	3.9	3.7	3.7
CO_2	Experimental	16.7	17.1	17.1
	Numerical	15.9	16.5	16.2

Table 6. Operating conditions for validation proposes and respective results.

- A more detailed devolatilization approach should be attempted.
- In addition, tar decomposition and chemical reactions for ash and some light hydrocarbons were not included.
- Ideal gas principles apply for the gases.
- Syngas is only formed by H_2, CO, CO_2, and C_nH_m and it is at chemical equilibrium.
- Heat losses from the components are neglected.

Some of these simplifications were corrected when the model was expended to deal with the heterogeneity of MSW as will be shown in the next subsection.

4.2. Model validation for PMSW

As stated in the mathematical model, to cope with the heterogeneity of MSW, the devolatilization model had to be restructured. Ideally, one would like to validate the new upgraded model with the experimental setup used earlier. However, due to unfortunate logistical and bureaucratic setbacks this was not possible.

To work around the problem, it was decided to validate the model using data collected from the literature [30]. **Table 7** shows the operating conditions used to validate the numerical model.

Figure 2 shows the comparison of the composition of obtained gas, estimated by the model, with that measured in the experiments.

Comparison between **Figure 2** and **Table 6** shows that the advancement in the model allowed a more complex system to perform in a similar manner and in some cases to predict syngas

Run	1	2	3	4	5	6	7	8	9
Temperature (°C)	493	705	602	507	687	593	691	593	507
MSW admission (Kg/h)	2.3	3	3	3	4	4	6	6	6
ER	0.5	0.4	0.4	0.4	0.3	0.3	0.2	0.2	0.2
Preheated air (°C)	290	352	296	281	352	307	352	308	279

Table 7. Operating conditions for the experimental gasification runs [30].

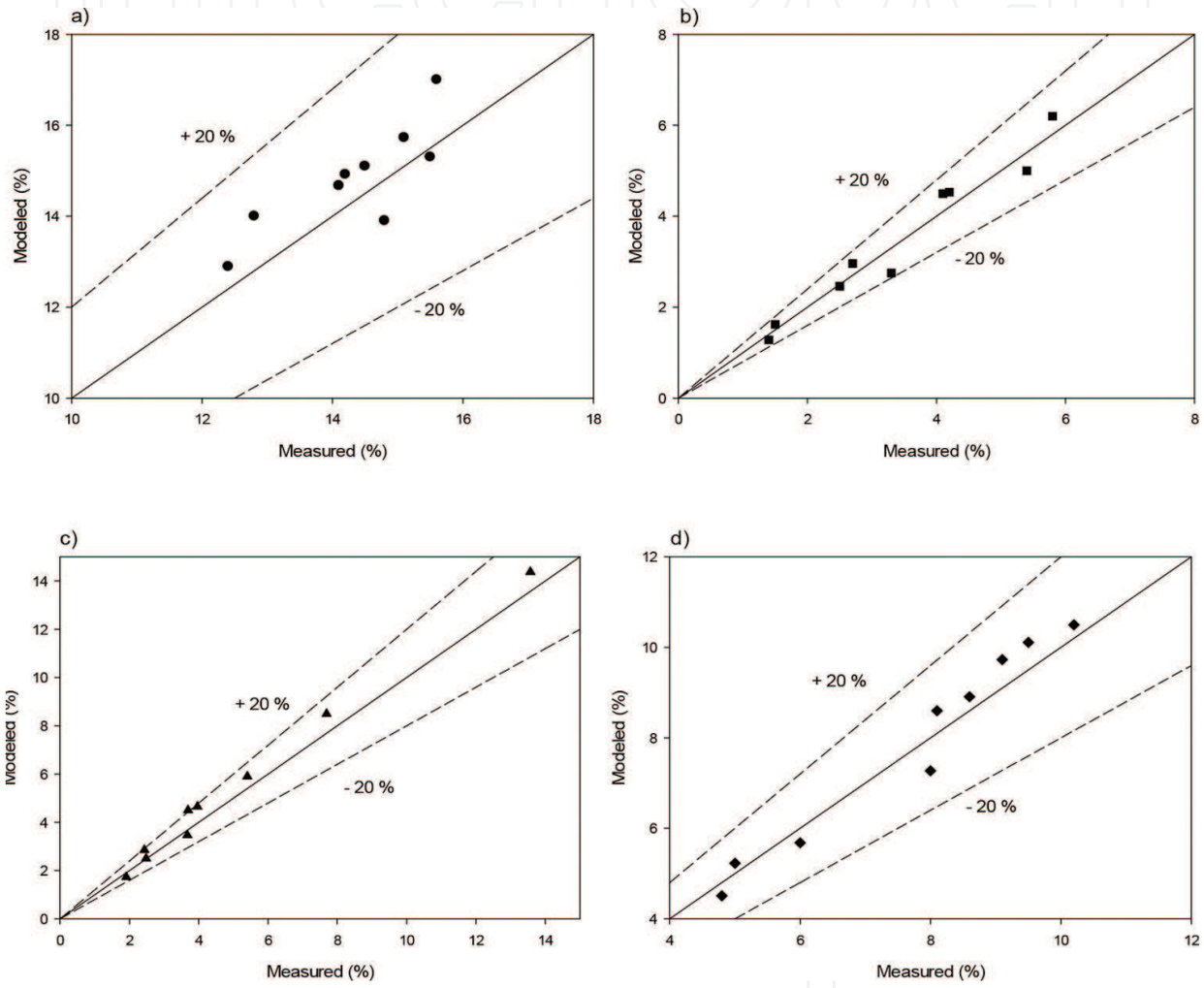

Figure 2. Comparison of the modeled and measured composition for (a) CO_2, (b) H_2, (c) C_nH_m, and (d) CO.

composition slightly better. This was due to a more realistic devolatilization model and the inclusion of light hydrocarbons.

4.3. Assessment of operational conditions

When scrutinizing a system (whatever it may be) it is imperative to devote a significant effort determining the influence of the main parameters on the system's output. In fact, the aim of the present subsection is to analyze the influence of several gasifier operating conditions including

equivalence ratio (ER), steam-to-biomass ratio (SBR), carbon dioxide-to-biomass (CO_2/B) ratio, and reactor temperature on the obtained gas composition.

4.3.1. Equivalent ratio

Perhaps the most common, and the most analyzed, parameter regarding the gasification process is the air flow rate. Air is the cheapest gasifying agent but it also produces the poorest gas because it is highly diluted in N_2 [31]. To solve this problem, pure oxygen can be used to obtain a much higher quality gas (since no nitrogen will be present or at least a much lower fraction). However, implementation is only possible through high investment causing uncertainty when it comes to large facilities [32].

Furthermore, the O_2content in an air mixture can sometimes be misleading due to nitrogen dilution and the effects of small variations on substrate admission in the syngas composition going unnoticed, hence our decision to study ER. ER is one of the most significant parameters, which have effect on the gasification process including syngas composition. In accordance with previous gasification studies [33], the equivalence ratio can be defined as:

$$\mathrm{ER} = \frac{\text{oxygen mass/dry MSW mass}}{\text{stoichiometric oxygen/MSW ratio}} \tag{4}$$

The ratio was maintained between 0.15 and 0.35 since all of the experiments conducted to validate the model must be in this range and also because the ER values most suitable for gasification found in the current literature range between 0.2 and 0.4 [34].

The model predictions for the described reactor about the influence of ER on syngas molar fraction are shown in **Figure 3**.

A quick analysis shows that increasing ER suppresses the formation of combustible gases (H_2, CO, and C_nH_m) while promoting the formation of CO_2 contents. Since increasing the ER leads to more inert gas to enter the reactor, the obtained gas will be more diluted in nitrogen resulting in a poorer gas. A decrease in H_2 and CO can also be explained by a decrease in the residence time, considering that as air flow rate increases, it is no longer sufficient for CO and H_2 formation reactions to occur. Although to a smaller degree, ER negatively affects the C_nH_m content by enhancing steam reactions at higher temperatures leading to methane decomposition [35]. Finally, carbon dioxide fraction is expected to increase since combustion reactions (that consume CO and H_2 to produce CO_2) will be promoted. Results are consistent with the current literature [36, 37].

Despite presenting similar trends, studied substrates exhibit significant differences in the relative syngas molar fraction. One may explain this difference by recurring to the fuel's chemical composition. As demonstrated by Silva et al. [15], higher biomass calorific values result in higher calorific syngas production. This relationship between the biomass calorific content and the syngas lower heating values (LHV) can be explained considering, first, that the biomass calorific value is related to the amount of carbon (C) and hydrogen (H) present in the biomass, and second, a larger amount of these two elements allows production of larger quantities of hydrogen and carbon monoxide, the major contributors for the calorific value of

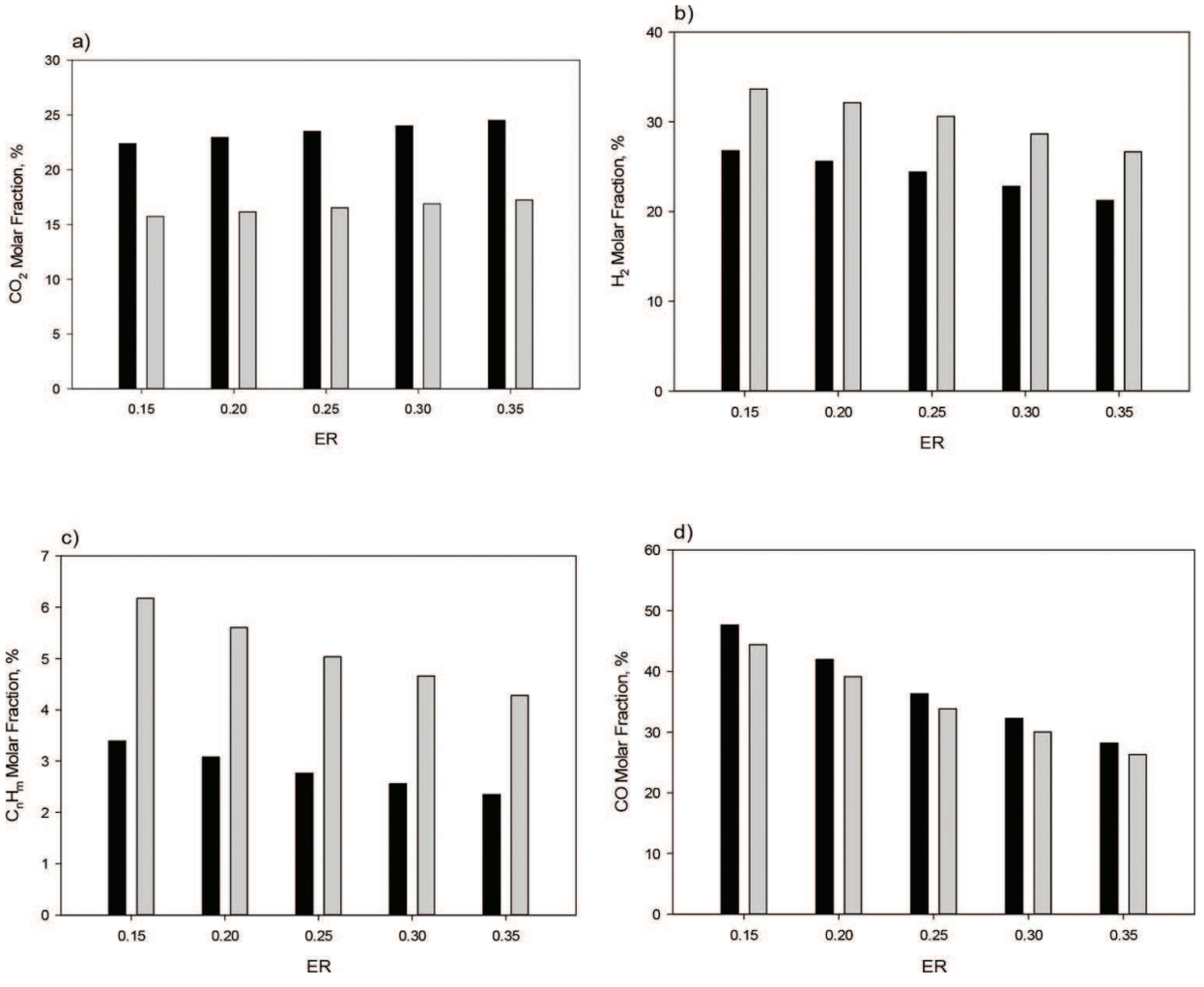

Figure 3. Comparison between PMSW (black columns) and forest residues (gray columns) as a function of ER for (a) CO_2, (b) H_2, (c) C_nH_m, and (d) CO (operating conditions: fuel feed rate = 25 kg/h; gasification temperature = 750°C).

the syngas. Nevertheless, since there are other biomass properties that can greatly influence the gasification process one must not take these conclusions as absolutes.

4.3.2. Steam-to-biomass ratio

Among oxidizing agents, steam gasification has received special attention since it produces a fuel gas with medium lower heating values of 12–18 MJ/Nm^3 [38], which is considerably higher than those from air gasification, while being less costly than oxygen gasification.

Steam-to-biomass ratio (SBR) is used in order to emphasize the effects of small variations on biomass admission, which often go unnoticed [39]. The SBR can be defined as the steam mass flow rate divided by the fuel mass flow rate (dry basis):

$$\text{SBR} = \frac{\text{Steam mass flow rate}}{\text{Biomass substrate mass flow rate}} \tag{5}$$

http://dx.doi.org/10.5772/65857

The SBR was varied over a range of values from 0 to 2 by holding the other variables constant. The range was selected based on previous findings from our research team using the same facilities (**Figure 4**).

An increase in SBR leads to an increase in H_2 and CO_2 and a decrease in CO and C_nH_m. SBR will mostly favor char and tar steam reforming as well as the water-gas shift reaction, which in turn will lead to an increase in CO_2 and H_2 content at the expense of CO and C_nH_m. In fact, according to Hernández et al. [40], for steam gasification, the water-gas shift reaction will dominate over the Boudouard one and CO will be consumed to produce CO_2 and H_2. These results are consistent with the current literature [41].

An increase in the CH_4 content relates to the decrease in oxidation of volatile matter, which is not balanced out by the consumption of CH_4 in the reforming reactions. These reactions have lower rates than oxidation ones but are most favored by low temperatures. However, at higher steam levels, the steam reforming can in fact shift CH_4 consumption will also be affected.

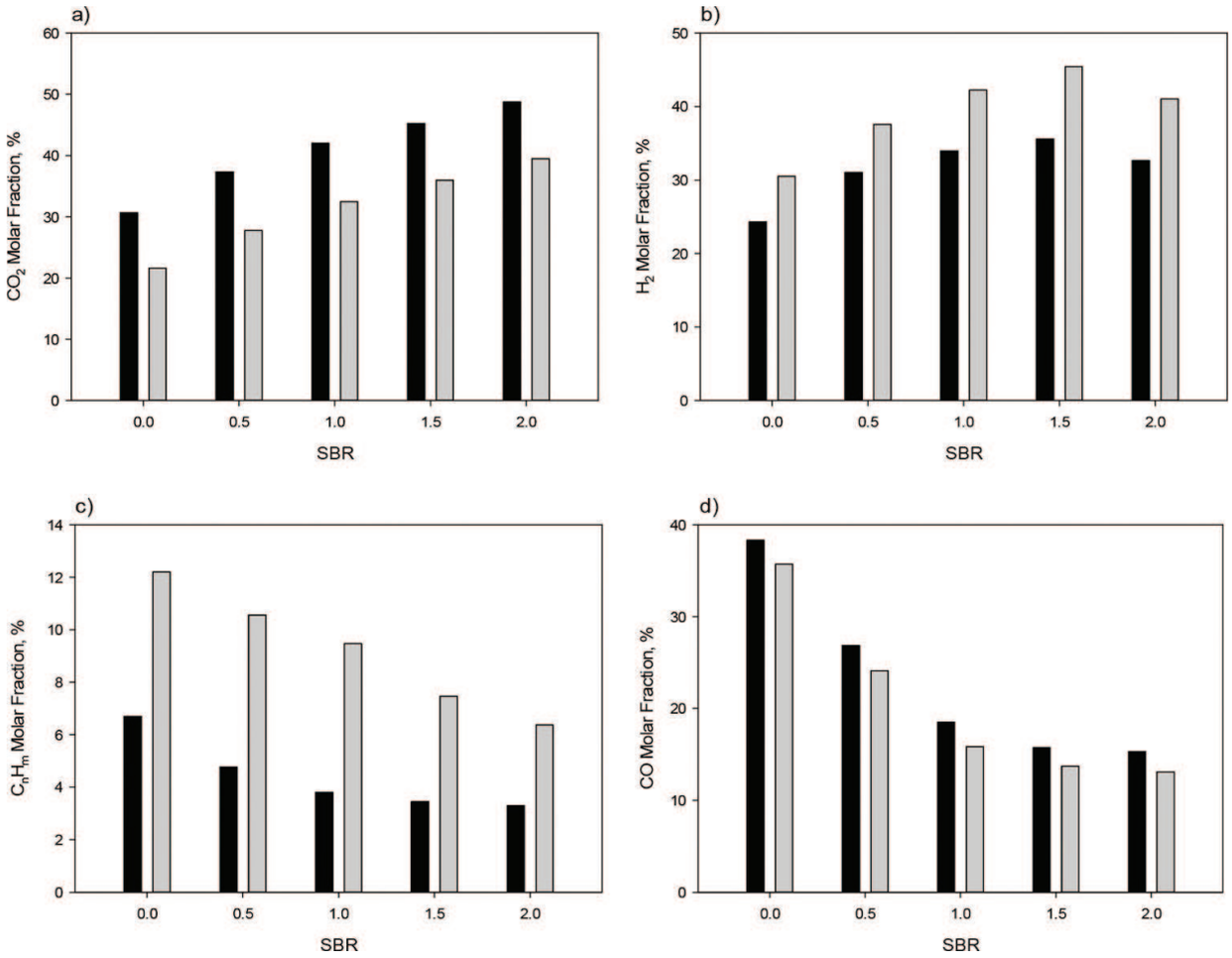

Figure 4. Comparison between PMSW (black columns) and forest residues (gray columns) as a function of SBR for (a) CO_2, (b) H_2, (c) C_nH_m, and (d) CO (operating conditions: fuel feed rate = 25 kg/h; gasification temperature = 750°C).

Excessive steam intake will lead to a significant decrease in gasification temperature, which in turn will have a negative effect on endothermic reactions, impairing product generation, which explains the decrease in H_2 after SBR=1.5, and producing insufficient heat to promote steam reforming and primary water-gas reactions. Furthermore, excessive steam could shift the steam reforming and water-gas reactions backward, consuming CO and H_2 to produce CO_2 and H_2O [42].

4.3.3. Carbon dioxide-to-biomass ratio

Even though steam gasification presents several advantages over air gasification, there are still some associated setbacks, such as the consumption of H_2O, which is an increasingly scarce resource.

Although poorly studied, carbon dioxide as a gasifier agent has been showing promising results, for starters, it consumes an unwanted end product (CO_2) of various industrial processes [43]. Furthermore, it also enhances both char gasification and pyrolysis and has the ability to act as a catalyst to enhance the thermal cracking of volatiles leading to tar mitigation.

The effect of carbon dioxide as a gasifying agent was studied using carbon dioxide-to-biomass ratio. The ratio was varied over a range of values from 0 to 1 by maintaining the other variables constant. To the best of our knowledge, regarding MSW, this ratio has only been investigated by our team [24], although some work has been published using biomass substrates by other researchers [44–46].

Results from **Figure 5** show that an increase in CO_2/B promotes the formation of CO and CO_2 while suppressing H_2 and C_nH_m. This can be explained with the fact that a higher CO_2 content mainly promotes Boudouard and reverse water-gas shift reactions, which leads to increase in CO fraction while H_2 decreases. On the other hand, C_nH_m molar fraction slightly decreases due to being consumed via CH_4reforming to produce CO and H_2 [47]. CO_2 content increases since a considerable fraction of the gasifying agent leaves the reactor unreacted.

Despite no results in the literature were found for MSW, those available for biomass are in agreement with the obtained results [44, 45, 48].

4.3.4. Gasification temperature

Gasification temperature is one of the most influential factors affecting the product gas composition and respective properties. The main reactions of the gasification are endothermic and thus strengthened by increasing temperature. Since the steam reforming, Boudouard, water-gas, and water-gas shift reactions occur simultaneously, the contents and ratios of considered species in the product gas are affected by temperature and partial pressures of reactants. Therefore, the reactor temperature significantly influences the syngas compositions. **Figure 6** show the influence of reactor temperature on final syngas composition for both substrates.

According to the Le Chatelier's principle, an increase in gasification temperature will favor products in endothermic reactions. Furthermore, promotion of endothermic reactions will lead to an increase in CO and H_2 content formation while decreasing CO_2 and C_nH_m [49].

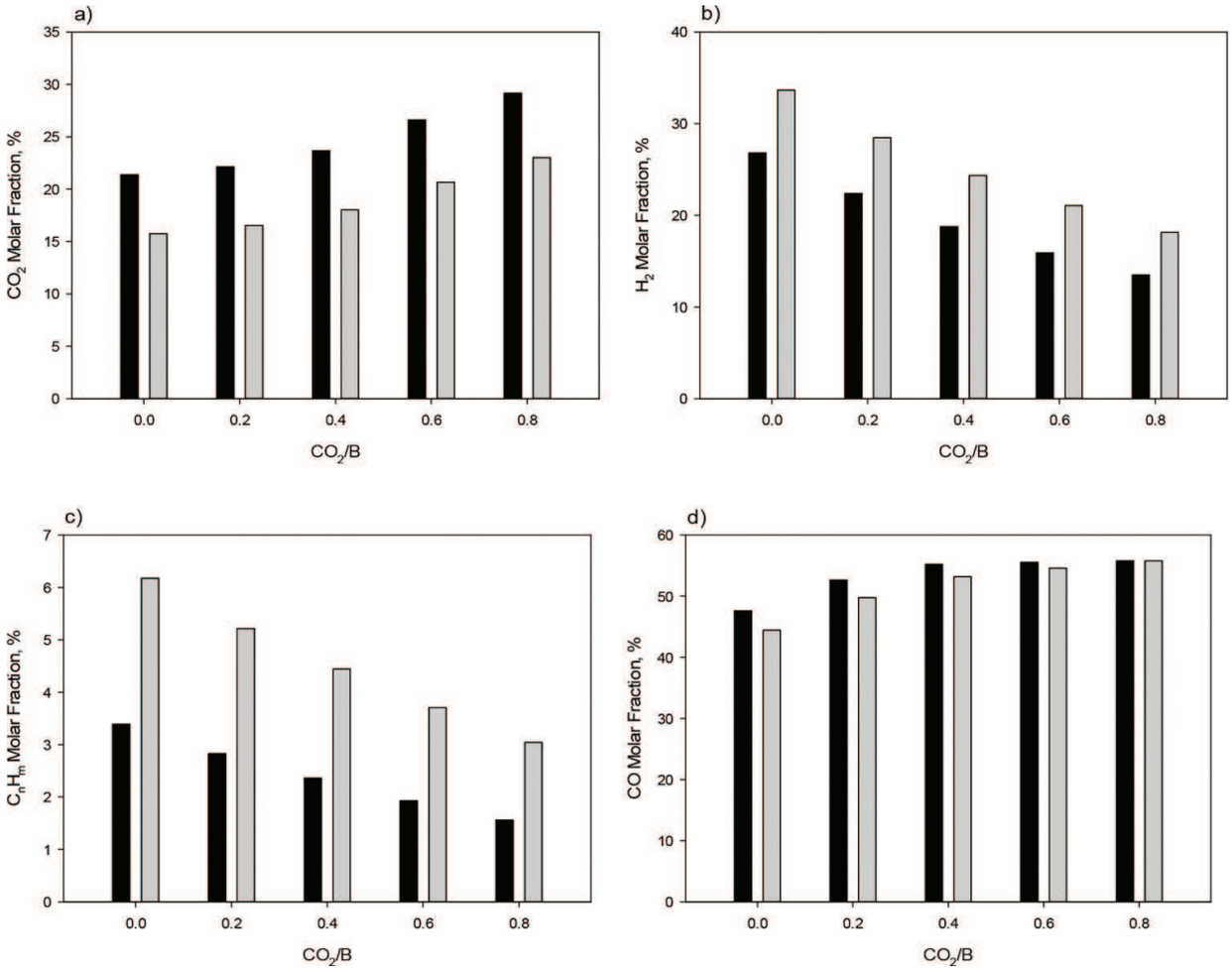

Figure 5. Comparison between PMSW (black columns) and forest residues (gray columns) as a function of CO_2/B for (a) CO_2, (b) H_2, (c) C_nH_m, and (d) CO (operating conditions: fuel feed rate = 25 kg/h; gasification temperature = 750°C).

Careful analysis shows that above 750°C hydrogen production becomes less pronounced while carbon monoxide further increases. In fact, in this range, the standard Gibbs free energy of the Boudouard reaction (responsible for CO production) becomes less than that of the water-gas reaction (main responsible for hydrogen production at lower temperatures), meaning that the former dominates over the latter as temperature increases. This is in agreement with the current literature [50].

Comparison between substrates was intentionally not discussed in the two previous subsections. The reason behind it is simply that all operating conditions share the same trends when it comes to different substrates, the underlining key is the biomass properties themselves.

4.4. Syngas quality indices

Syngas quality indices such as CH_4/H_2 and H_2/CO not only give a good indication of process efficiency, but also give its most suitable application. For instances, syngas with high CH_4/H_2 ratios tends to be used in domestic purposes while high H_2/CO ratios tend to be preferred in the chemical industry [51].

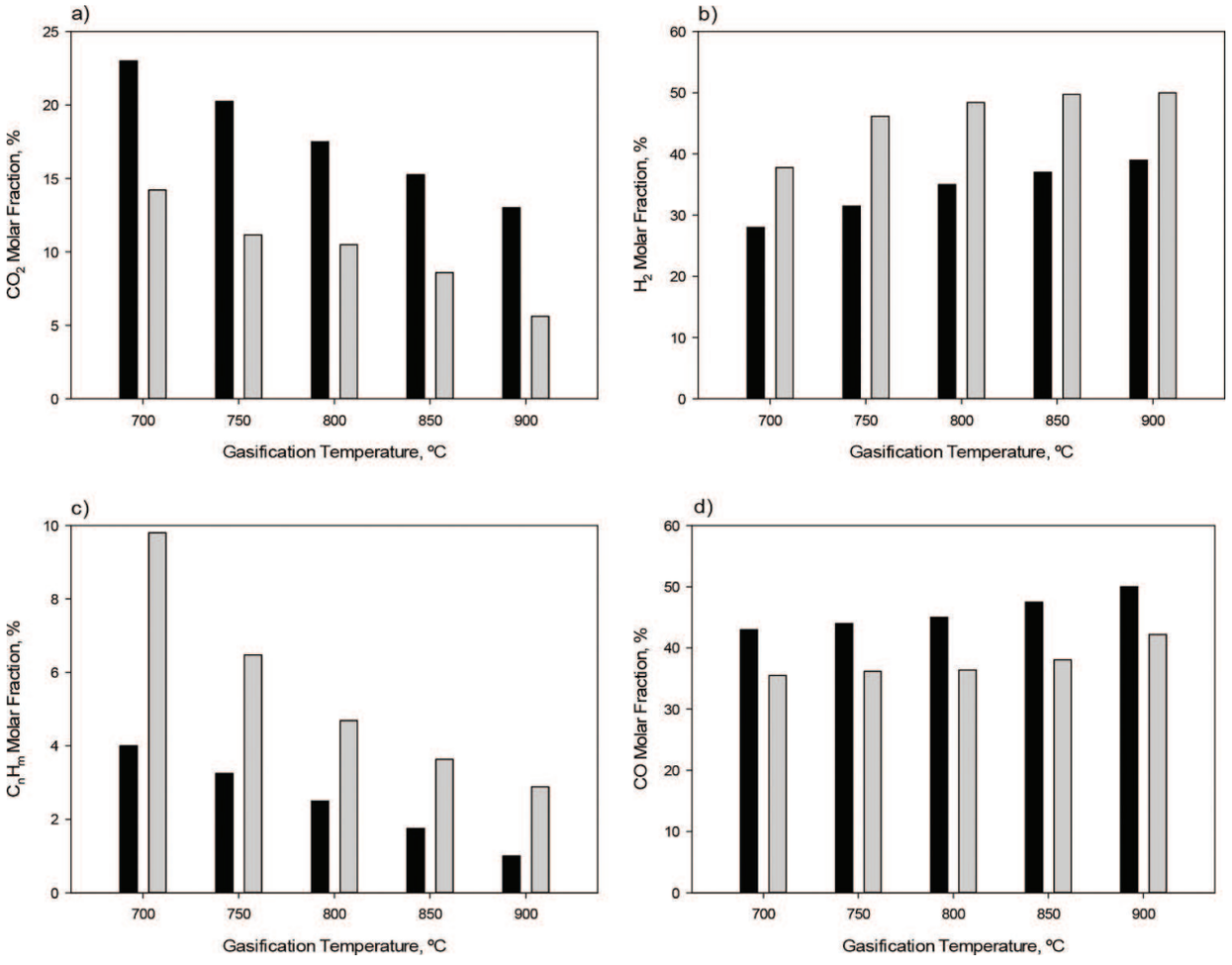

Figure 6. Comparison between PMSW (black columns) and forest residues (gray columns) as a function of gasification temperature for (a) CO_2, (b) H_2, (c) C_nH_m, and (d) CO. Dry and N_2-free basis (operating conditions: ER – 0.25; SBR – 1; CDMR – 0.4; MSW admission – 25 kg/h).

Besides syngas quality indices, there are other gasification products that can help determine process quality, namely carbon conversion (CC), cold gas efficiency (CGE), and tar content.

4.4.1. Methane-to-hydrogen ratio

Figure 7 displays the effect of gasification temperature on the syngas CH_4/H_2 ratio using the operating conditions from **Figure 6**.

Figure shows that the CH_4/H_2 ratio suffers a steep decrease with an increase in temperature. As can be seen from **Figure 6** (and corresponding explanation), an increase in gasification temperature will promote the formation of H_2. Meanwhile, due to the strengthening of the endothermic steam-methane reactions a decrease in CH_4 fraction is also expected.

At higher temperatures, usually above 800°C, one may notice that ratio decrease becomes less pronounced. This can be explained with the fact that, simply because within the studied

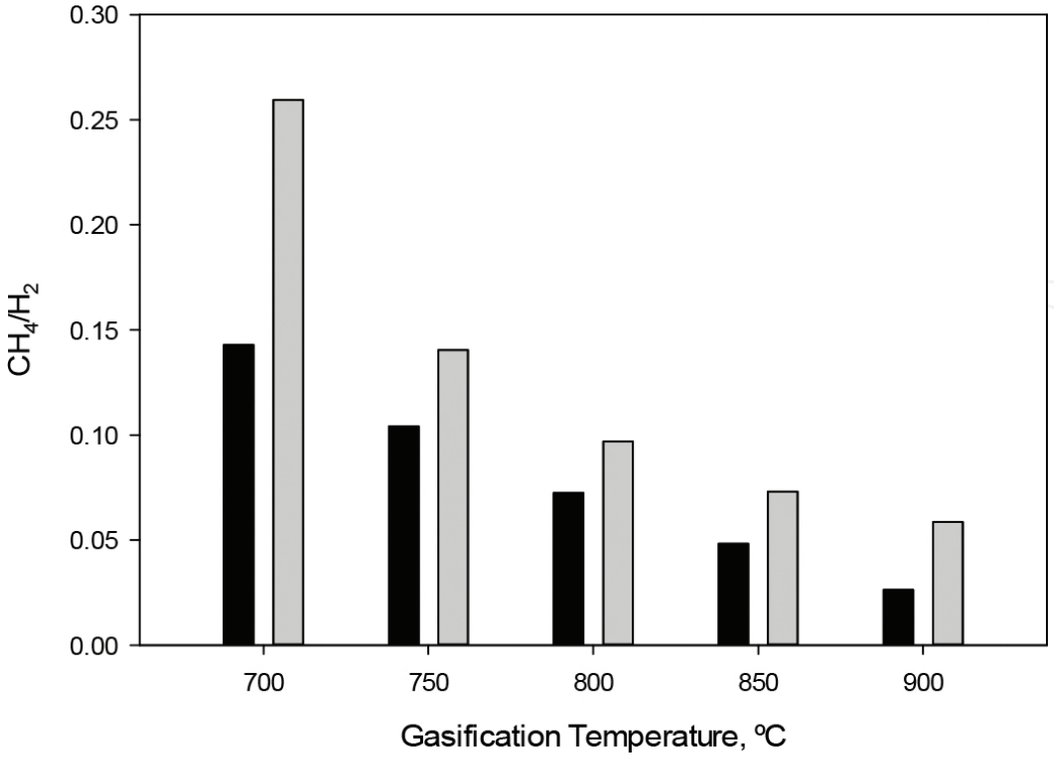

Figure 7. Syngas CH_4/H_2 ratio as a function of the gasification temperature for PMSW (black columns) and forest residues (gray columns) (dry and N_2-free basis).

temperature range, a decrease in CH_4 is somewhat constant while at higher temperature hydrogen production will also be less pronounced [33].

Forest residues presented a higher CH_4/H_2 ratio, especially for lower temperatures. Pinpointing exactly why this is can be extremely challenging due to a number of biomass properties that influence the gasification process. One can argue that since forest residues have a higher carbon and hydrogen content (according to our data, if we consider the proximate analysis as received from PMSW, C content is just 33.66 and H 4.42%) which will lead to more combustible gases. Furthermore, an increase in the CH_4 content is related to higher levels of volatile matter, which also might explain why forest residues present the higher ratio.

4.4.2. Hydrogen-to-carbon monoxide ratio

As estimated by Butterman and Castaldi [43], the H_2/CO ratio has an obvious impact on the ideal application for a given substrate. Higher H_2/CO ratios permit for the operation of solid oxide fuel cells (SOFC) [52] while medium H_2/CO ratios are suitable for FT synthesis of liquid fuels. Mid-to-lower ratios are mainly appropriate for catalyst-based FT synthesis while very low ratios are particularly appropriate for the production of a specific biomass-derived liquid chemical [53].

Figure 8 displays the effect of gasification temperature on the syngas H_2/CO ratio using the operating conditions from **Figure 6**.

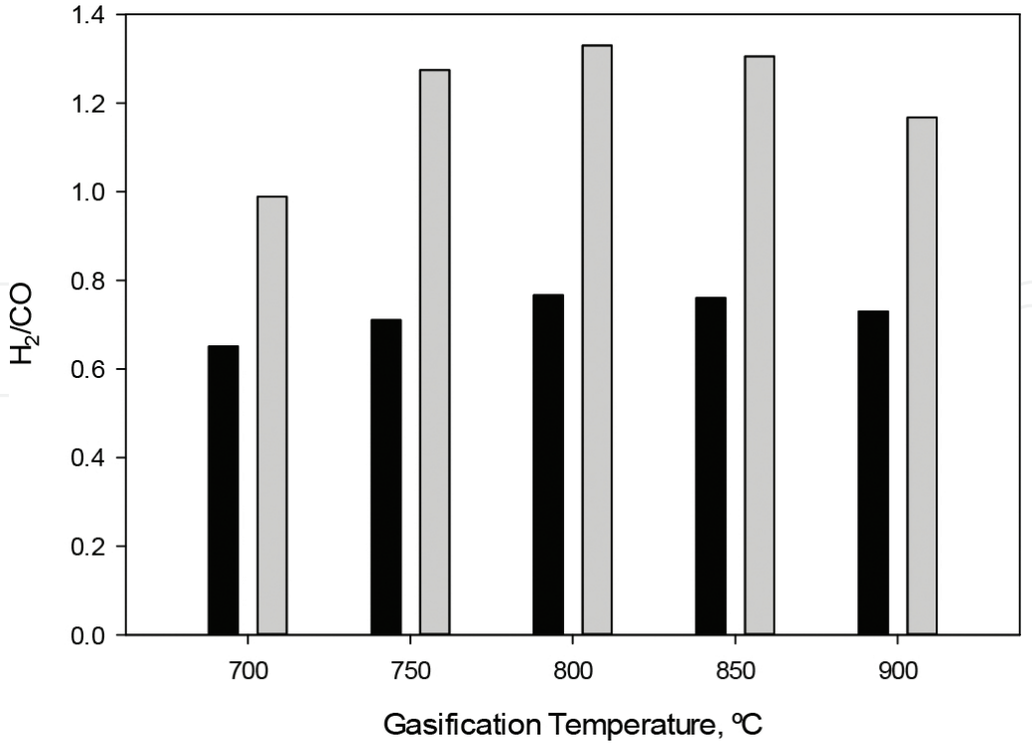

Figure 8. Syngas H_2/CO ratio as a function of the gasification temperature for PMSW (black columns) and forest residues (gray columns) (dry and N_2-free basis).

Conversely to CH_4/H_2, the H_2/CO ratio presents two distinct trends: from 700 to 800°C, gasification temperature has a positive influence on the H_2/CO ratio whereas an increase beyond 800°C shows the opposite trend. This can be explained with the fact that at low temperatures H_2 production is enhanced by primary water-gas reaction as well as steam-methane reforming reactions while at higher temperatures primary water-gas as well as Boudouard reaction will favor CO production.

Perhaps most importantly, in the range between 750 and 800°C, the standard Gibbs free energy of the Boudouard reaction (responsible for CO production) becomes less than that of the water-gas reaction (main responsible for hydrogen production at lower temperatures), indicating that the former dominates over the latter as temperature increases, leading to a decrease in the H_2/CO ratio, which is in agreement with the literature [54].

To make it useful for the chemical industry to synthesize products such as methanol and virgin naphtha, H_2/CO ratios higher than 1.70 should be presented, which neither of these two substrates were able to achieve, although forest residues were able to reach close to 1.4. The H_2/CO ratio would be increased by an injection of water [51].

4.4.3. Carbon conversion

Carbon conversion can be defined by the fraction of carbon from the substrate converted into carbon in syngas composition, and can give an good indication of the amount of unconverted

http://dx.doi.org/10.5772/65857

materials, thus providing a measure of chemical efficiency of the process. It can be expressed as:

$$\text{Carbon Conversion} = \frac{12 \times M}{X_c \times m} \tag{6}$$

where M stands for the total molar flow rate of carbon in syngas composition, X_c stands for the carbon fraction in the MSW, and m stands for the MSW flow rate into the gasifier.

Figure 9 displays the effect of gasification temperature on carbon conversion using the operating conditions from **Figure 6**.

Figure shows that gasification temperature has a positive effect on carbon conversion. Higher temperatures will favor tar reforming leading to an increase in gas yield and carbon conversion [55]. Furthermore, an increase in temperature enhances steam reforming reactions, which in turn promote carbon conversion [41].

Although operational conditions were kept constant to ensure uniform residence time, substrates with different size particles lead to different residence times [47, 52]. In addition, the increasing residence time promotes gasification and carbon conversion reactions, leading to a higher gas yield [53]. Since forest residues have a smaller particle it leads to higher carbon conversion values.

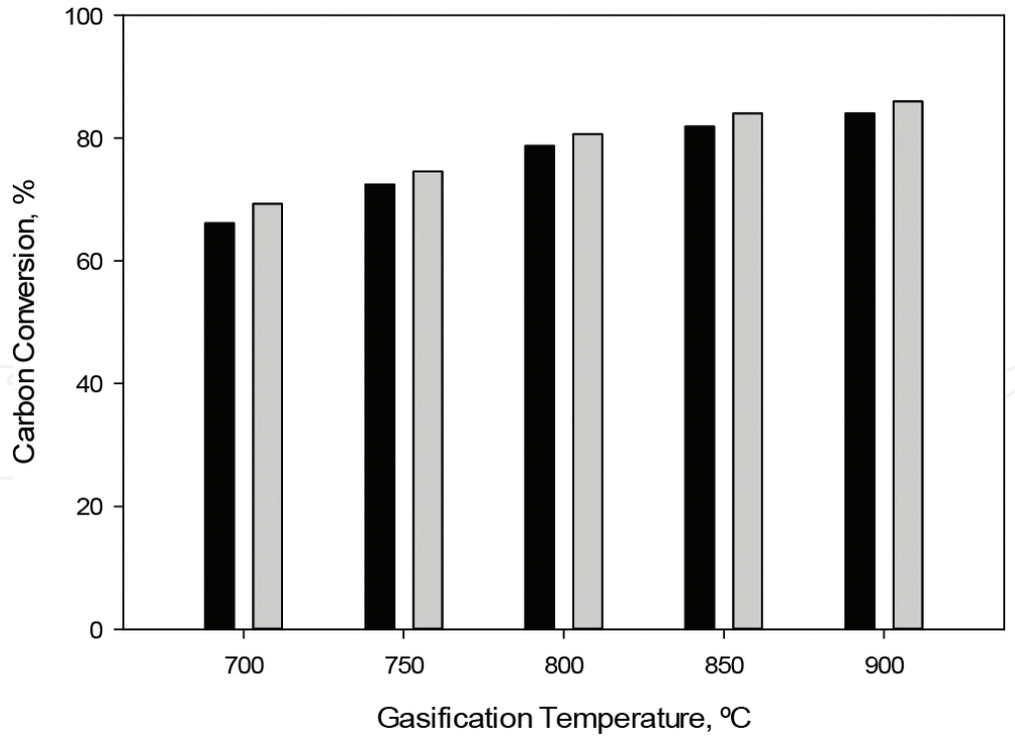

Figure 9. Carbon conversion as a function of the gasification temperature for PMSW (black columns) and forest residues (gray columns) (dry and N_2-free basis).

4.4.4. Cold gas efficiency

CGE can be defined as the percentage of the heating value of MSW converted into the heating value of the product gas. It can be computed as follows:

$$\mathrm{CGE} = \frac{\text{Gas yield} \times \text{HHV of product gas}}{\text{HHV of fuel} + \text{Heat addition}} \tag{7}$$

Figure 10 displays the effect of gasification temperature on CGE using the operating conditions from **Figure 6**.

Similarly to CC, gasification temperature also has a positive influence on CGE. This is expected since the main gasification reactions are endothermic and thus strengthened by increasing temperature as well as gas yield, the two main factors responsible for CGE increase. Results are in agreement with the current literature [56, 57].

As expected, the calculated CGE for MSW is significantly lower due to a combination of low gas yield and poor syngas LHV. Efficiency values for both forest residues and MSW are within range from what is commonly found in the current literature [58].

4.4.5. Tar content

One of the major problems to deal with during biomass gasification is tar formation. At reduced temperature, tar condenses, blocking and fouling process equipment (such as engines

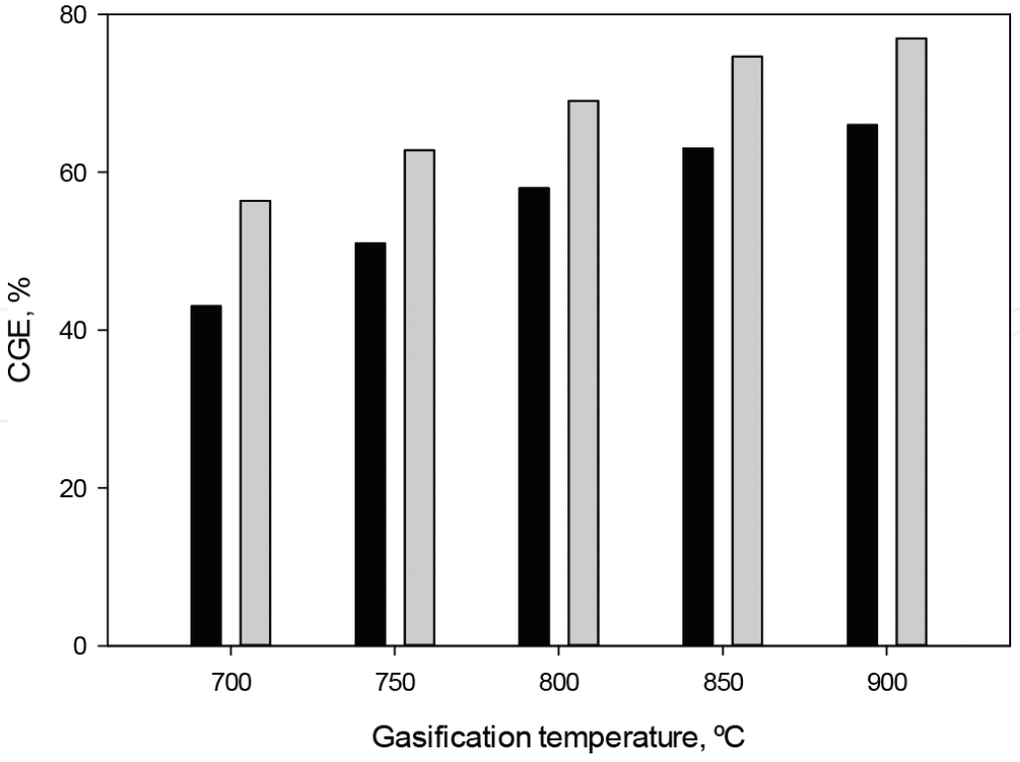

Figure 10. CGE as a function of the gasification temperature for PMSW (black columns) and forest residues (gray columns) (dry and N_2-free basis).

and turbines). According to Devi et al. [59], tar should be prevented or eliminated in the gasifier by manipulating factors such as operating conditions, addition of active bed materials, and possible reactor design modifications.

Figure 11 displays the effect of gasification temperature on the tar content using the operating conditions from **Figure 6**.

Figure shows that gasification temperature strongly influences the tar content. This can be explained with the fact that a high temperature favors destruction and reforming of tar, leading to a decrease in tar content [60].

As previously mentioned, a higher volatile content leads to an increase in residence time that, in turn, favors gasification reactions [61]. According to Aljbour and Kawamoto [62], an increase in residence time can lead to a reduction in the tar content. Since forest residues have a slightly higher volatile content, it comes with no surprise that it also consist a slightly lower tar content.

4.5. Process optimization

As shown all throughout the paper, gasification parameters have a strong influence on the overall process quality. Trying to have a better understanding of the underpinning mechanisms requires performing several gasification runs studying different operating conditions and parameters. Without a systematic approach such as the design of experiments this can become extremely time-consuming as well as expensive. Combining optimization methodologies such as the DoE with numerical models avoids expensive and time-consuming

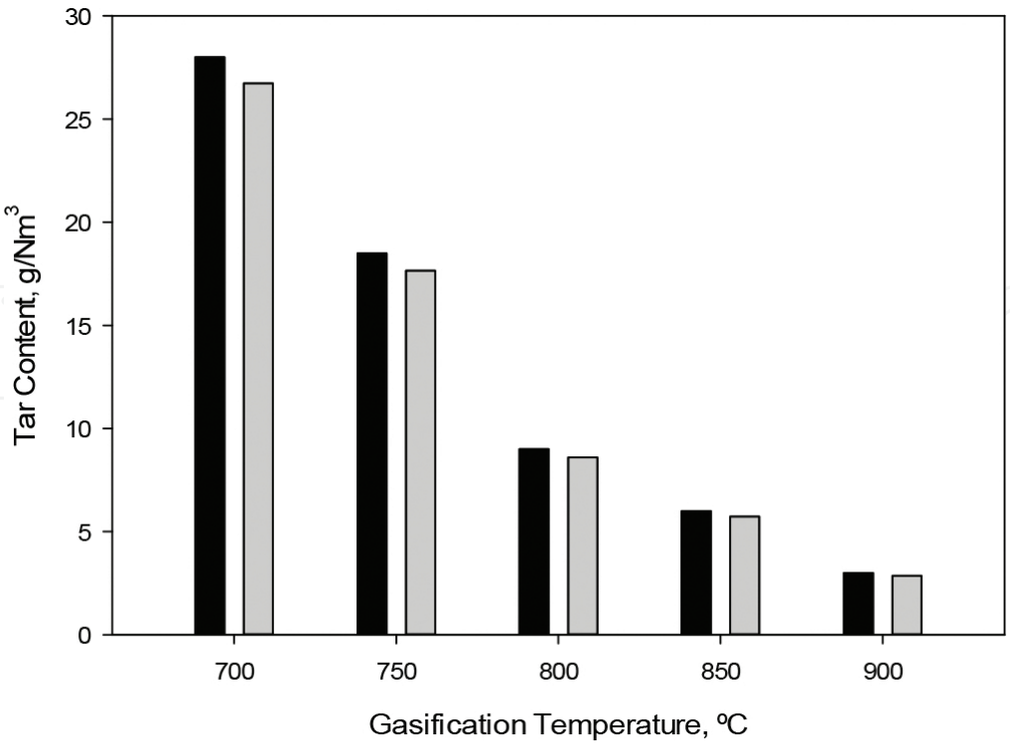

Figure 11. Tar content as a function of the gasification temperature for PMSW (black columns) and forest residues (gray columns) (dry and N_2-free basis).

experiments while obtaining the optimal operational condition set according to the desired response [63].

To test this hypothesis, an exergy efficiency optimization model was built using data obtained from the numerical model. The optimization model aimed to establish where the maximum exergy efficiency is according to the substrate and operating conditions chosen.

Particularly, in order to promote a more hydrogen-rich gas, the optimization model focused on an exergy flow rate of the produced hydrogen instead of syngas.

The empirical model was built minimizing the sum of the residues square to give the parameters of a second-order response model.

$$Y = B_0 + \sum_{i=1}^{3} B_i \times X_i + \sum_{i=1}^{3} B_{i,i} \times X_i^2 + \sum_{j=2}^{3}\sum_{i<j}^{3} B_{i,j} \times X_i \times X_j \tag{8}$$

where Y is the response, the X_i terms are the main factors $(-1 \leq X_i \leq 1)$, temperature (1), steam-to-biomass ratio (2), and biomass type (3) and the B_i terms are the equation coefficients related to the main factors. The B_0 term is the interception coefficient, the $B_{i,i}$ terms are the quadratic effects (give the curvature to the response surface), and the $B_{i,j}$ terms symbolize the cross-interactions between factors. The present design does not consider the use of replicates because the results are obtained by computer simulations. In this case, a test on lack of fit and analysis concerning pure error are not provided [64]. Despite these circumstances much of the standard statistical analyses remain relevant, including measurements of model-fit such as PRESS (predicted residual sum of squares).

ANOVA analysis with high values for PRESS and "R-squared predicted" (not shown) also reinforced that the exergy efficiency response is well described by the empirical model in the design space.

Figures 12 and **13** show the hydrogen exergy efficiency as a function of the temperature and SBR for MSW and forest residues, respectively.

Similarly to what was shown in previous subsections, both substrates present very similar trends. In general, hydrogen efficiency increases with SBR since adding steam increases its chemical energy and exergy content. However, adding steam also demands additional exergy.

Regarding influence of gasification temperature one can clearly see that it has a positive effect on hydrogen efficiency all throughout the studied range. This can be explained by an increase in gas yield and enthalpy of gas component [56, 65].

The interpolating polynomial indicated in Eq. (8) provides the maximum values for hydrogen efficiency for both studied substrates. The maximum efficiency value was found at 900°C with a SBR of 1.5 for MSW and 1 for forest residues, with respective values of 50.6 and 50.2%.

Surprisingly, forest residues and MSW presented virtually the same maximum hydrogen efficiency. This can be explained with forest residues having the higher hydrogen molar composition and the higher gas yield, while MSW presenting the lower substrate exergy value,

http://dx.doi.org/10.5772/65857

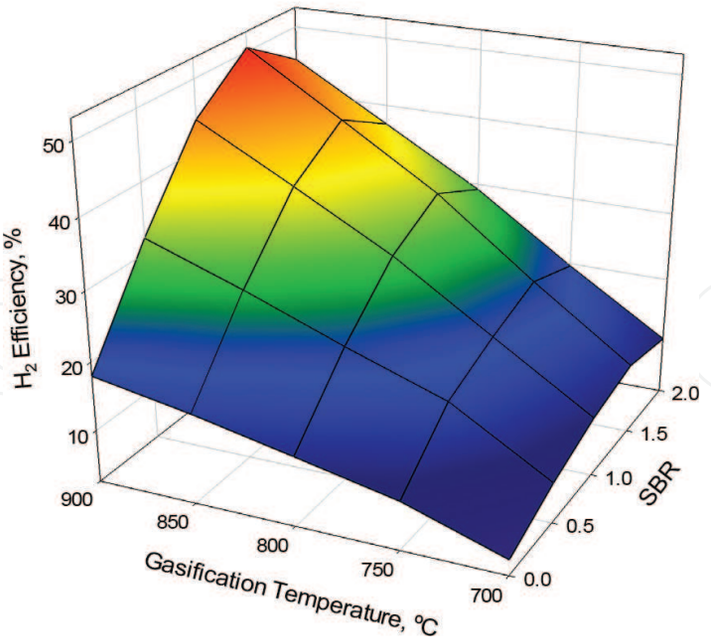

Figure 12. Hydrogen exergy efficiency as a function of the temperature and SBR for MSW.

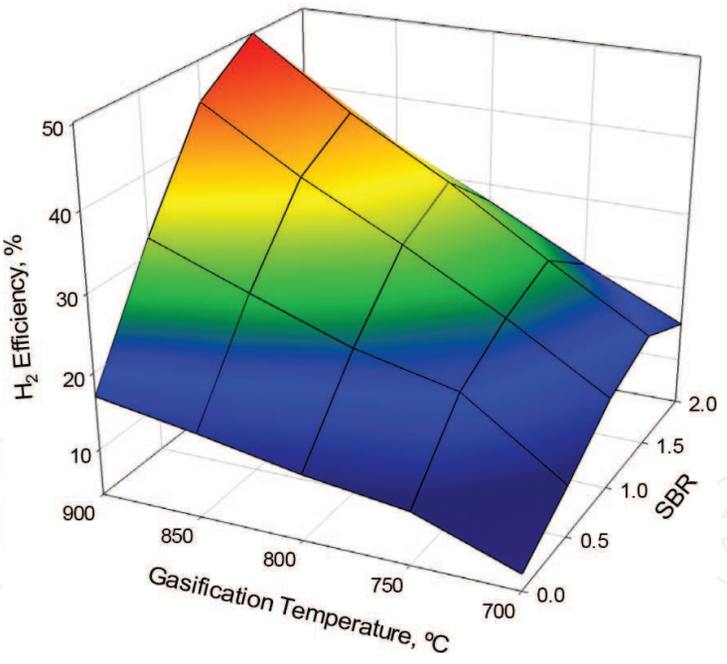

Figure 13. Hydrogen exergy efficiency as a function of temperature and SBR for forest residues.

leading to the latter having a slightly higher maximum hydrogen exergy value. Perhaps more important is the fact that forest residues have a much higher C_nH_m fraction (which is much more calorific than H_2 or CO), leading to a substantially higher CGE. When considering hydrogen efficiency, we are only considering hydrogen fraction and gas yield, so higher hydrocarbons do not influence the results. Available literature supports the conclusions made in this study [56, 65].

Even though results from MSW were not on par with those from forest residues in regard to CGE, exciting results were seen in both tar content and hydrogen efficiencies.

4.6. Role of numerical simulation in research assistance

Most real-life problems are simply not solved by analytical methods, especially if they involve interaction between physical processes or when comparison is made with real-experimental data. The use of numerical simulation is becoming increasingly imperative with the increase in computing power available by allowing researchers to get results not achievable by other means.

Most simulators of physical phenomena nowadays are using numerical methods rather than closed-form solutions. Examples would be solvers for Maxwell's equations (electromagnetic phenomena), Navier-Stokes equations (fluid mechanics), Schrödinger's equation (quantum mechanics), Fourier equations (heat conduction), and so on. Even "simple" simulators like the SPICE circuit simulator use numerical methods for nearly all but the simplest resistor circuits.

Numerical solutions open new possibilities for analysis but solutions can sometimes be difficult to interpret. Furthermore, simulators such as fluent are not 100% accurate or certain to give the user a physically real answer, one still has to know the basic physics to even setup most such simulators and one needs to know something about numerical analysis to know how and why such methods typically fail to simulate if you want identify or debug simulation failures.

The key determining factor is the level of complexity the researcher is willing to take (in other words what computational cost is the researcher willing to take). In the presented work, there were several choices that were necessary to make in order to ensure work feasibility:

- What kind of geometry simplifications could one make without jeopardizing physical model?
- What would the optimal grid density be? A very courser mesh could lead to very poor results, but a very fine mesh could mean dozens or even hundreds of hours extra just to improve results by a few percentage points.
- Is it better to use faster approaches like PDF flamelet models even though their fundamental assumption of infinitely fast chemistry renders them inapplicable for modeling low-Btu, low-exit velocity flaring?
- Using a radiation model can definitely improve the simulation results but requires a considerable amount of additional computational time, is it worth?
- When using a chemistry set, some authors opt to use detailed mechanisms (sometimes containing hundreds of reactions and dozens of species), while others prefer to use reduced or even simplified versions.

These are just a small fraction of all choices necessary to make when dealing with such a complex system as the one described in Section 3. Depending on system complexity, even with all the necessary adjustments to ensure faster convergence, some simulations will require optimal planning and patience. Some known examples by ANSYS:

- NETL fluidization challenge problem, able to simulate 16 s of flow time per day on 12 processors with a complete particle size distribution (PSD);
- Flow of solids in a riser, approximately 1 s of flow time simulated in a day in a single processor.

However, all this effort is rewarded when researchers are able to apply their results in creating credible model descriptions of new systems, which can be used in new designs or to improve the parameters on working systems and decision making for its modernization.

Nevertheless, perhaps the greatest benefit of using numerical models is the impact that these can bring not only for industrial purposes but also in important areas such as financial, social, and environmental areas.

5. Conclusions

Ideally, researchers would always want to test their hypothesis using the latest equipment in the most advanced laboratories with a large team of experts available to assist them. However, only an insignificant fraction has access to such conditions, and even those who do still have to go through tedious bureaucratic and logistical setbacks. Numerical simulation methods are used to study the behavior of systems whose mathematical models are too complex to provide analytical solutions in a time and cost-efficient way.

In this chapter, one of the most challenging energetic systems to predict was analyzed, the gasification process. In fact, gasification is considered to be one of the most difficult processes to model due to the chemical and physical interactions that occur throughout. A previously developed numerical model was used and its results validated using data collected from the literature and from a semiindustrial gasifier. Forest residues (one of the most abundant substrates in Portugal) and municipal solid wastes (one of the greatest challenges facing modern society) were analyzed. The model able not only to satisfactory the experimental results but also to correctly predict the trends of all studied parameters.

Finally, the numerical model was coupled with an optimization model designed to predict the optimal operation conditions for obtaining a more hydrogen-rich gas. This further states the ability of numerical simulations not only to assist analyzing the key trends of a given process but also how they can be used to predict the optimal operating point for a given optimal response.

Nomenclature

A, B	calibration constants
A_i	preexponential factor
$C_{1\varepsilon}$, $C_{2\varepsilon}$, $C_{3\varepsilon}$	constants
C_p	specific heat capacity
D_0	diffusion rate coefficient

E_i	activation energy
G_k	generation of turbulence kinetic energy due to the mean velocity gradients
G_b	generation of turbulence kinetic energy due to buoyancy
h_q	specific enthalpy of phase
h_{pq}	heat transfer coefficient between the fluid phase and the solid phase
k	thermal conductivity
Nu	Nusselt number
$\dot{m}$	biomass flow entering into the gasifier
M	total mole flow of carbon in the syngas components
M_i	molecular weight of each the species
M_c	molecular weight
$M_{w,i}$	molecular weight of i component
p	gas pressure
Pr	Prandtl number
p_s	particle phase pressure due to particle collisions
$\vec{Q}_{pq}$	heat transfer between p^{th} and q^{th} phases
$\vec{q}_q$	heat flux
q^{th}	specific enthalpy
R	universal gas constant
R_i	net generation rate of specie i due to homogeneous reaction
Re	Reynolds number
R_c	reaction rate
S_i	source term of the species i production from the solid heterogeneous reaction
S_k	user-defined source terms
S_q	source term due to chemical reactions
$S\varepsilon$	user-defined source terms
T	temperature
t_s	particle phase stress tensor
U	mean velocity
v	instantaneous velocity
X_C	carbon fraction in the biomass (obtained from the ultimate analysis)
Y	mass fraction
Y_M	contribution of the fluctuating dilatation in compressible turbulence to the overall dissipation rate

Other symbols

α	volume fraction
β	gas-solid interphase drag coefficient
γ_c	stoichiometric coefficient
γ_{Θ_a}	collisional dissipation of energy
ε	dissipation rate
ρ	density

φ_{ls}	energy exchange between gas and solid phases
k_{Θ_a}	diffusion coefficient
$k_{\Theta_a}\nabla(\Theta_s)$	diffusion energy
$(-p_s\bar{I} + \bar{\tau}_s) : \nabla(\vec{v}_s)$	generation of energy by the solid stress tensor.
τ	tensor stress
μ	viscosity

Subscripts

g gas phase
s solid phase
i component

Acknowledgements

We would like to express our gratitude to the Portuguese Foundation for Science and Technology (FCT) for the support to the grant SFRH/BD/86068/2012 and the project PTDC/EMS-ENE/6553/2014 as well as IF/01772/2014. We also would like to thank Dr. Paulo Brito for providing experimental data needed to complete this paper.

Author details

Nuno Couto and Valter Silva*

*Address all correspondence to: vsilva@inegi.up.pt

INEGI-FEUP, Faculty of Engineering, University of Porto, Porto, Portugal

References

[1] V. Silva, E. Monteiro, A. Rouboa, An analysis on the opportunities, technology and potential of biomass residues for energy production in Portugal, in: A. Méndez-Vilas (Ed.) Materials and Processes for Energy, Formatex Research Center, Spain 2013, pp. 190–201.

[2] W.C. Tuckenger, Renewable energy technologies, in: U.W. UNDP (Ed.) World Energy Assessment of the United Nations, USA 2000, pp. 219–272.

[3] U. Arena, Process and technological aspects of municipal solid waste gasification. A review, Waste Management, 32 (2012) 625–639.

[4] G. del Alamo, A. Hart, A. Grimshaw, P. Lundstrøm, Characterization of syngas produced from MSW gasification at commercial-scale ENERGOS Plants, Waste Management, 32 (2012) 1835–1842.

[5] M. Lapuerta, J.J. Hernández, A. Pazo, J. López, Gasification and co-gasification of biomass wastes: Effect of the biomass origin and the gasifier operating conditions, Fuel Processing Technology, 89 (2008) 828–837.

[6] S. Ferreira, N.A. Moreira, E. Monteiro, Bioenergy overview for Portugal, Biomass and Bioenergy, 33 (2009) 1567–1576.

[7] D. Baruah, D.C. Baruah, Modeling of biomass gasification: A review, Renewable and Sustainable Energy Reviews, 39 (2014) 806–815.

[8] F. Tabet, I. Gökalp, Review on CFD based models for co-firing coal and biomass, Renewable and Sustainable Energy Reviews, 51 (2015) 1101–1114.

[9] S. Kraft, M. Kuba, F. Kirnbauer, K. Bosch, H. Hofbauer, Optimization of a 50 MW bubbling fluidized bed biomass combustion chamber by means of computational particle fluid dynamics, Biomass and Bioenergy, 89 (2016) 31–39.

[10] M. Siedlecki, W. De Jong, A.H.M. Verkooijen, Fluidized bed gasification as a mature and reliable technology for the production of bio-syngas and applied in the production of liquid transportation fuels: A review, Energies, 4 (2011) 389.

[11] G. Mirmoshtaghi, H. Li, E. Thorin, E. Dahlquist, Evaluation of different biomass gasification modeling approaches for fluidized bed gasifiers, Biomass and Bioenergy, 91 (2016) 69–82.

[12] R.I. Singh, A. Brink, M. Hupa, CFD modeling to study fluidized bed combustion and gasification, Applied Thermal Engineering, 52 (2013) 585–614.

[13] D.M. Snider, S.M. Clark, P.J. O'Rourke, Eulerian–Lagrangian method for three-dimensional thermal reacting flow with application to coal gasifiers, Chemical Engineering Science, 66 (2011) 1285–1295.

[14] Q. Xue, R.O. Fox, Multi-fluid CFD modeling of biomass gasification in polydisperse fluidized-bed gasifiers, Powder Technology, 254 (2014) 187–198.

[15] V. Silva, E. Monteiro, N. Couto, P. Brito, A. Rouboa, Analysis of syngas quality from Portuguese biomasses: An experimental and numerical study, Energy & Fuels, 28 (2014) 5766–5777.

[16] N. Couto, V. Silva, E. Monteiro, S. Teixeira, R. Chacartegui, K. Bouziane, P.S.D. Brito, A. Rouboa, Numerical and experimental analysis of municipal solid wastes gasification process, Applied Thermal Engineering, 78 (2015) 185–195.

[17] N. Couto, V. Silva, E. Monteiro, P. Brito, A. Rouboa, Using an Eulerian-granular 2-D multiphase CFD model to simulate oxygen air enriched gasification of agroindustrial residues, Renewable Energy, 77 (2015) 174–181.

[18] S. Teixeira, E. Monteiro, V. Silva, A. Rouboa, Prospective application of municipal solid wastes for energy production in Portugal, Energy Policy, 71 (2014) 159–168.

[19] Z.A.B.Z. Alauddin, P. Lahijani, M. Mohammadi, A.R. Mohamed, Gasification of lignocellulosic biomass in fluidized beds for renewable energy development: A review, Renewable and Sustainable Energy Reviews, 14 (2010) 2852–2862.

[20] N. Couto, V. Silva, E. Monteiro, P.S.D. Brito, A. Rouboa, Experimental and numerical analysis of coffee husks biomass gasification in a fluidized bed reactor, Energy Procedia, 36 (2013) 591–595.

[21] M.J.V. Goldschmidt, J.A.M. Kuipers, W.P.M. van Swaaij, Hydrodynamic modelling of dense gas-fluidised beds using the kinetic theory of granular flow: Effect of coefficient of restitution on bed dynamics, Chemical Engineering Science, 56 (2001) 571–578.

[22] P. Cornejo, O. Farías, Mathematical modeling of coal gasification in a fluidized bed reactor using a Eulerian granular description. International Journal of Chemical Reactor Engineering 9 (1) 2011.

[23] N. Couto, V. Silva, A. Rouboa, Assessment on steam gasification of municipal solid waste against biomass substrates, Energy Conversion Management 124 (15) 2016.

[24] N. Couto, V. Silva, A. Rouboa, Municipal solid waste gasification in semi-industrial conditions using air-CO2 mixtures, Energy, 104 (2016) 42–52.

[25] S. Badzioch, P.G.W. Hawksley, Kinetics of thermal decomposition of pulverized coal particles, Industrial & Engineering Chemistry Process Design and Development, 9 (1970) 521–530.

[26] O. Onel, A.M. Niziolek, M.M.F. Hasan, C.A. Floudas, Municipal solid waste to liquid transportation fuels – Part I: Mathematical modeling of a municipal solid waste gasifier, Computers & Chemical Engineering, 71 (2014) 636–647.

[27] S.J. Gelderbloom, D. Gidaspow, R.W. Lyczkowski, CFD simulations of bubbling/collapsing fluidized beds for three Geldart Groups, AIChE Journal, 49 (2003) 844–858.

[28] N. Couto, V.B. Silva, C. Bispo, A. Rouboa, From laboratorial to pilot fluidized bed reactors: Analysis of the scale-up phenomenon, Energy Conversion and Management, 119 (2016) 177–186.

[29] V. Silva, A. Rouboa, Combining a 2-D multiphase CFD model with a response surface methodology to optimize the gasification of Portuguese biomasses, Energy Conversion and Management, 99 (2015) 28–40.

[30] G. Xiao, B.-S. Jin, Z.-P. Zhong, Y. Chi, M.-j. Ni, K.-F. Cen, R. Xiao, Y.-J. Huang, H. Huang, Experimental study on MSW gasification and melting technology, Journal of Environmental Sciences, 19 (2007) 1398–1403.

[31] M. Campoy, A. Gómez-Barea, F.B. Vidal, P. Ollero, Air–steam gasification of biomass in a fluidised bed: Process optimisation by enriched air, Fuel Processing Technology, 90 (2009) 677–685.

[32] K. Maniatis, Progress in biomass gasification: An overview, in: Progress in Thermochemical Biomass Conversion, Blackwell Science Ltd., United Kingdom 2008, pp. 1–31.

[33] N.D. Couto, V.B. Silva, E. Monteiro, A. Rouboa, Assessment of municipal solid wastes gasification in a semi-industrial gasifier using syngas quality indices, part 1, Energy, 93 (2015) 864–873.

[34] L. Wang, C.L. Weller, D.D. Jones, M.A. Hanna, Contemporary issues in thermal gasification of biomass and its application to electricity and fuel production, Biomass and Bioenergy, 32 (2008) 573–581.

[35] Z. Wang, T. He, J. Qin, J. Wu, J. Li, Z. Zi, G. Liu, J. Wu, L. Sun, Gasification of biomass with oxygen-enriched air in a pilot scale two-stage gasifier, Fuel, 150 (2015) 386–393.

[36] S.S. Thanapal, K. Annamalai, J.M. Sweeten, G. Gordillo, Fixed bed gasification of dairy biomass with enriched air mixture, Applied Energy, 97 (2012) 525–531.

[37] N. Couto, E. Monteiro, V. Silva, A. Rouboa, Hydrogen-rich gas from gasification of Portuguese municipal solid wastes, International Journal of Hydrogen Energy, 41 (2016) 10619–10630.

[38] P. McKendry, Energy production from biomass (part 3): Gasification technologies, Bioresource Technology, 83 (2002) 55–63.

[39] Q. Miao, J. Zhu, S. Barghi, C. Wu, X. Yin, Z. Zhou, Modeling biomass gasification in circulating fluidized beds: Model sensitivity analysis, International Journal of Energy and Power Engineering, 2 (2013) 57.

[40] J.J. Hernández, G. Aranda, J. Barba, J.M. Mendoza, Effect of steam content in the air–steam flow on biomass entrained flow gasification, Fuel Processing Technology, 99 (2012) 43–55.

[41] J. Wang, G. Cheng, Y. You, B. Xiao, S. Liu, P. He, D. Guo, X. Guo, G. Zhang, Hydrogen-rich gas production by steam gasification of municipal solid waste (MSW) using NiO supported on modified dolomite, International Journal of Hydrogen Energy, 37 (2012) 6503–6510.

[42] C. Franco, F. Pinto, I. Gulyurtlu, I. Cabrita, The study of reactions influencing the biomass steam gasification process, Fuel, 82 (2003) 835–842.

[43] H.C. Butterman, M.J. Castaldi, CO2 as a carbon neutral fuel source via enhanced biomass gasification, Environmental Science and Technology, 43 (2009) 9030–9037.

[44] T. Renganathan, M.V. Yadav, S. Pushpavanam, R.K. Voolapalli, Y.S. Cho, CO_2 utilization for gasification of carbonaceous feedstocks: A thermodynamic analysis, Chemical Engineering Science, 83 (2012) 159–170.

[45] L. Garcia, M.L. Salvador, J. Arauzo, R. Bilbao, CO_2 as a gasifying agent for gas production from pine sawdust at low temperatures using a Ni/Al coprecipitated catalyst, Fuel Processing Technology, 69 (2001) 157–174.

[46] A.M. Parvez, I.M. Mujtaba, T. Wu, Energy, exergy and environmental analyses of conventional, steam and CO_2-enhanced rice straw gasification, Energy, 94 (2016) 579–588.

[47] O. Corigliano, P. Fragiacomo, Technical analysis of hydrogen-rich stream generation through CO_2 reforming of biogas by using numerical modeling, Fuel, 158 (2015) 538–548.

[48] Y. Cheng, Z. Thow, C.-H. Wang, Biomass gasification with CO_2 in a fluidized bed, Powder Technology, 296 (2016) 87–101.

[49] C. Loha, P.K. Chatterjee, H. Chattopadhyay, Performance of fluidized bed steam gasification of biomass – Modeling and experiment, Energy Conversion and Management, 52 (2011) 1583–1588.

[50] T. Song, J. Wu, L. Shen, J. Xiao, Experimental investigation on hydrogen production from biomass gasification in interconnected fluidized beds, Biomass and Bioenergy, 36 (2012) 258–267.

[51] P. De Filippis, C. Borgianni, M. Paolucci, F. Pochetti, Prediction of syngas quality for two-stage gasification of selected waste feedstocks, Waste Management, 24 (2004) 633–639.

[52] M. Marco, M. Giovanni, P. Lorenzo, R. Rosario, A quasi-3D computer model of a planar SO fuel cell stack, in: 3rd International Energy Conversion Engineering Conference, American Institute of Aeronautics and Astronautics, San Francisco, CA 2005.

[53] X. Peng, B. Toseland, A. Wang, G. Parris, Progress in development of LPDME process: Kinetics and catalysts, in: Coal Liquefaction & Solid Fuels Contractors Review Conference, Pittsburgh, Pennsylvania, 1997.

[54] J. Xiao, L.H. Shen, X. Deng, Z.M. Wang, X.L. Zhong, Study on characteristics of pressurized biomass gasification, Zhongguo Dianji Gongcheng Xuebao/Proceedings of the Chinese Society of Electrical Engineering, 29 (2009) 103–108.

[55] S. Luo, B. Xiao, Z. Hu, S. Liu, X. Guo, M. He, Hydrogen-rich gas from catalytic steam gasification of biomass in a fixed bed reactor: Influence of temperature and steam on gasification performance, International Journal of Hydrogen Energy, 34 (2009) 2191–2194.

[56] Y. Zhang, B. Li, H. Li, B. Zhang, Exergy analysis of biomass utilization via steam gasification and partial oxidation, Thermochimica Acta, 538 (2012) 21–28.

[57] Y. Wu, W. Yang, W. Blasiak, Energy and exergy analysis of high temperature agent gasification of biomass, Energies, 7 (2014) 2107.

[58] K.J. Ptasinski, M.J. Prins, A. Pierik, Exergetic evaluation of biomass gasification, Energy, 32 (2007) 568–574.

[59] L. Devi, K.J. Ptasinski, F.J.J.G. Janssen, A review of the primary measures for tar elimination in biomass gasification processes, Biomass and Bioenergy, 24 (2003) 125–140.

[60] X. Zhang, S. Deng, J. Wu, W. Jiang, A sustainability analysis of a municipal sewage treatment ecosystem based on energy, Ecological Engineering, 36 (2010) 685–696.

[61] F. Pinto, R.N. André, C. Carolino, M. Miranda, P. Abelha, D. Direito, N. Perdikaris, I. Boukis, Gasification improvement of a poor quality solid recovered fuel (SRF). Effect of using natural minerals and biomass wastes blends, part B, Fuel, 117(2014) 1034–1044.

[62] S.H. Aljbour, K. Kawamoto, Bench-scale gasification of cedar wood – Part II: Effect of operational conditions on contaminant release, Chemosphere, 90 (2013) 1501–1507.

[63] V. Silva, A. Rouboa, Optimizing the gasification operating conditions of forest residues by coupling a two-stage equilibrium model with a response surface methodology, Fuel Processing Technology, 122 (2014) 163–169.

[64] M.J. Anderson, P.J. Whitcomb, RSM Simplified: Optimizing Processes Using Response Surface Methods for Design of Experiments, Productivity Press, New York, 2005.

[65] A. Abuadala, I. Dincer, Efficiency evaluation of dry hydrogen production from biomass gasification, Thermochimica Acta, 507–508 (2010) 127–134.